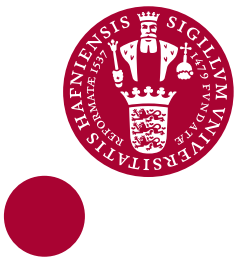

Spatiotemporal dynamics of phosphorus release, oxygen consumption and greenhouse gas emissions after localised soil amendment with organic fertilisers

Christel, Wibke; Zhu, Kun; Hoefer, Christoph; Kreuzeder, Andreas; Santner, Jakob; Bruun, Sander; Magid, Jakob; Jensen, Lars Stoumann

Published in:
Science of the Total Environment

DOI:
10.1016/j.scitotenv.2016.02.152

Publication date:
2016

Document version
Publisher's PDF, also known as Version of record

Science of the Total Environment 554–555 (2016) 119–129

Contents lists available at ScienceDirect

Science of the Total Environment

journal homepage: www.elsevier.com/locate/scitotenv

Spatiotemporal dynamics of phosphorus release, oxygen consumption and greenhouse gas emissions after localised soil amendment with organic fertilisers

Wibke Christel [a,c], Kun Zhu [a,f], Christoph Hoefer [b], Andreas Kreuzeder [b,d], Jakob Santner [b,e], Sander Bruun [a], Jakob Magid [a], Lars Stoumann Jensen [a,*]

[a] Department for Plant and Environmental Sciences, University of Copenhagen, Thorvaldsensvej 40, 1871 Frederiksberg C, Denmark
[b] Rhizosphere Ecology and Biogeochemistry Group, Department of Forest and Soil Sciences, University of Natural Resources and Life Sciences, Vienna, Konrad-Lorenz-Strasse 24, 3430 Tulln, Austria
[c] Department of Commerce, Industry and Agriculture, Danish Environmental Protection Agency, 1401 Copenhagen C, Denmark
[d] Land Salzburg, Natur- und Umweltschutz, Gewerbe (Abteilung 5), Michael-Pacher-Straße 36, 5020 Salzburg, Austria
[e] Division of Agronomy, Department of Crop Sciences, University of Natural Resources and Life Sciences, Vienna, Konrad-Lorenz-Strasse 24, 3430 Tulln, Austria
[f] College of Resources and Environmental Sciences, China Agricultural University, Beijing 100193, PR China

HIGHLIGHTS

- Spatio-temporal dynamics of pig manure-derived P reacting with soil were monitored.
- Over time, P availability in manure solids decreased, but increased in manure char.
- CO_2 respiration in manure solids-amended soil was higher than in char-amended soil.
- Both, manure solids and char derived P remained very localised P sources.
- Hence, high P uptake efficiency depends on manure or char placement close to roots.

GRAPHICAL ABSTRACT

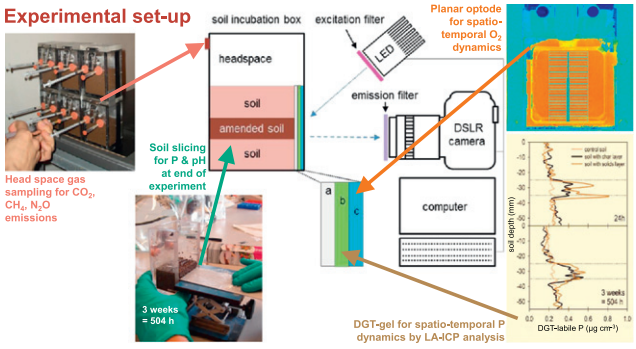

ARTICLE INFO

Article history:
Received 4 November 2015
Received in revised form 17 February 2016
Accepted 21 February 2016
Available online 4 March 2016

Editor: Simon Pollard

Keywords:
Fertiliser placement
Planar oxygen optode
Diffusive gradients in thin films (DGT)
Pig manure solids
Biochar

ABSTRACT

Organic fertilisation inevitably leads to heterogeneous distribution of organic matter and nutrients in soil, i.e. due to uneven surface spreading or inhomogeneous incorporation. The resulting localised hotspots of nutrient application will induce various biotic and abiotic nutrient turnover processes and fixation in the residuesphere, giving rise to distinct differences in nutrient availability, soil oxygen content and greenhouse gas (GHG) production. In this study we investigated the spatiotemporal dynamics of the reaction of manure solids and manure solids char with soil, focusing on their phosphorus (P) availability, as current emphasis on improving societal P efficiency through recycling waste or bio-based fertilisers necessitates a sound understanding of their behaviour. Soil layers amended at a constant P application rate with either pig manure solids or char made from pig manure solids were incubated for three weeks between layers of non-amended, P-depleted soil. Spatial and temporal changes in and around the amendment layers were simultaneously investigated in this study using a sandwich sensor consisting of a planar oxygen optode and multi-element diffusive gradients in thin films (DGT) gels, combined with GHG emission measurements. After three weeks of incubation, the soil containing a layer amended with manure solids had a lower overall O_2 content and had emitted significantly more CO_2 than the non-amended control or the

* Corresponding author.
E-mail address: lsj@plen.ku.dk (L.S. Jensen).

http://dx.doi.org/10.1016/j.scitotenv.2016.02.152

char-amended soil. The P availability from manure solids was initially higher than that from the char, but decreased over time, whereas from the char-amended layer P availability increased in the same period. In both treatments, increases in P availability were confined to the amended soil layer and did not greatly affect P availability in the directly adjacent soil layers during the three-week incubation. These results highlight the importance of placing organic P fertilisers close to where the plant roots will grow in order to facilitate optimal fertiliser use efficiency.

1. Introduction

The application of organic waste as a fertiliser is one means of improving nutrient recirculation within agricultural systems and can also reduce dependence on mineral fertiliser production and imports. Once applied, several essential plant nutrients contained in organic soil amendments have to be microbially mineralised before becoming plant available. Various mechanisms occurring simultaneously control organic matter turnover in soil (Lützow et al., 2006). Spatial inaccessibility and organo-mineral interactions govern organic matter stability in soils in the long term (Lützow et al., 2006). In the initial phase after organic matter amendment (weeks to months), the quality of the organic amendment, its spatial distribution in the soil and physicochemical soil properties control the decomposition rate and influence the amount of greenhouse gases released (Zhu et al., 2014). In organically amended soil, these processes controlling nutrient turnover and availability are expected to be highly variable both spatially and temporally.

The most intense mineralisation activity usually takes place in the residuesphere, the soil directly adjacent to and influenced by the decomposable amendment (Magid et al., 2006). The altered dynamics in oxygen (O_2) consumption, the release of plant available nutrients and GHG emissions are often limited to this soil region. However, the relevance of spatial heterogeneity in the organic matter addition is very rarely taken into consideration when these processes are studied. While different spatial patterns of organic fertiliser addition to soil have been investigated, most studies have focused on temporal trends of either GHG emissions (Wulf et al., 2002) or nutrient release (Magid et al., 2006), but rarely on both (Zhu et al., 2014). Moreover, mineralisation studies have mostly been limited to carbon (C) and nitrogen (N) mineralisation, although some organic amendments, such as the solid fraction of animal manure for example, constitute a considerable source of other essential plant nutrients, especially phosphorus (P) (Hjorth et al., 2010; Popovic et al., 2012). P mobility in soil is greatly limited due to the strong sorption of the phosphate ion to soil particle surfaces, but also due to the precipitation of Ca-, Fe-, and Al-phosphates (Hinsinger, 2001). Consequently it is well known that localised placement of readily available P fertiliser close to the plant roots can enhance plant uptake and efficiency due to reduced transport distance, improved root interception and reduced binding to soil minerals (Lu and Miller, 1993) and similar effects have been found for placement of animal manures by controlled injection (Schröder et al., 2015). The P content of organic amendments can be enriched through pyrolysis, for example, into biochar (Tsai et al., 2012; Christel et al., 2014), but P availability has been found to vary, depending on the thermal processing technique applied (Christel et al., 2014; Christel et al., in press). Moreover, chars have become an interesting soil amendment beyond merely being a means of C-sequestration or a nutrient source, as has been extensively discussed in recent literature (Spokas et al., 2012).

Solute imaging techniques have been used extensively in aquatic biogeochemistry over the last few decades, but they are relatively new to terrestrial soil research (Santner et al., 2015a). Diffusive gradients in thin films (DGT) (Davison and Zhang, 1994) and planar optode imaging techniques (Glud et al., 1996; Larsen et al., 2011) have recently been combined for the simultaneous imaging of trace metals and O_2 in marine sediments (Stahl et al., 2012) and in paddy field soils (Williams et al., 2014). In terrestrial ecosystems, chemical imaging of solutes at sub-mm resolutions has to date mainly been used to study the distributions of P, pH and enzyme activity in the root zone (Santner et al., 2012; Blossfeld et al., 2013; Spohn and Kuzyakov, 2014).

Advances in the development of thin (~100 μm), cation and anion-binding DGT gels (Kreuzeder et al., 2013) allow for the simultaneous application of DGT and oxygen optodes to map nutrient and O_2 distributions concomitantly in heterogeneous soil systems. Since GHG production and emissions may be influenced by the spatial and temporal dynamics of O_2 and nutrient availability, their simultaneous determination by classical headspace GHG measurements alongside optode and DGT mapping is a promising, novel approach to evaluating the effects of heterogeneously placed organic amendments on soil GHG and nutrient dynamics.

This study is the first to investigate both the temporal and spatial changes in soil O_2 levels and in the availability of P and potential trace metal contaminants in and around the residuesphere with simultaneous headspace measurement of CO_2, CH_4 and N_2O emissions. Manure solids and char, produced from manure solids, were used as labile and recalcitrant (i.e. more and less mineralisable) organic amendments respectively, and applied heterogeneously to a nutrient-depleted soil. It was hypothesised that: (i) soil O_2 is depleted in and around the residuesphere as the organic amendment decomposes, (ii) more GHGs are emitted from soil amended with labile manure solids than with recalcitrant char, and (iii) P availability increases in the soil layers adjacent to the residuesphere over time. Furthermore, the availability of potential trace metal contaminants, co-applied with the manure solids and the char, was monitored.

2. Materials and methods

The experimental set-up consisted of six identical soil incubation boxes, each equipped with septa for gas sampling and a removable front plate with a planar optode for monitoring soil O_2 levels and attaching DGT gels. Two manure-derived organic soil amendments – the solid fraction of pig slurry (referred to as 'solids') and biochar produced from the same manure solids (referred to as 'char') – were investigated and compared to a control treatment without amendment. The three treatments (solids, char and control) were prepared in duplicate incubation boxes.

2.1. Soil and organic amendments

The soil used in this experiment was collected from the plough layer of the long-term Nutrient Depletion Trial on the experimental farm of the University of Copenhagen in Taastrup, Denmark. This plot has been continuously used for crop production since 1964, only receiving nitrogen (N) fertiliser at a low rate but no other nutrients, resulting in a very low P status (Olsen-P = 10 mg kg^{-1} soil, c_{DGT} = approx. 45 μg PO_4-P L^{-1}). The soil was a carbonate-free, sandy clay loam (16.0% clay, 17.0% silt, 67.0% sand) with 1.15% organic carbon and 0.128% total nitrogen content, C/N of 9, a cation exchange capacity (CEC) of 8.4 cmol kg^{-1} (Christel et al., 2014) and pH_{CaCl_2} values of 6.9 (0.01 mol L^{-1} $CaCl_2$) and pH_{H_2O} of 7.4 (d.i. water). The soil was pre-moistened to 13.8% soil water content (the proportion of water mass to total bulk mass in wt%), passed through a 2-mm sieve and pre-incubated at room temperature (21 ± 3 °C) for two weeks prior to the experiment.

The solid fraction of pig slurry ('solids') and char, produced from the same solid fraction, were used as the organic fertiliser amendment. The solid fraction of pig slurry, separated using a decanter centrifuge, was sampled from a farm in Northern Denmark, stored frozen for several months and then dried at 80 °C. Before pyrolysis, the solid fraction was dried and pelleted. The pellets were pyrolised at laboratory scale at 600 °C with a char-yield of 38.4% (Christel et al., in press). The char pellets were crushed by hand and ground with a mortar before soil application. Properties of the solids and char is listed in Table 1, more detailed information on the separation process and elemental composition of the solid fraction can be found in Sommer et al. (2015). Further information on the pyrolysis and P availability in different soils over time can be found in Christel et al. (in press).

2.2. Incubation box design

The experimental mesocosms consisted of six identical, transparent acrylic glass boxes (inner dimensions: height 100 mm × length 60 mm × width 40 mm, with a headspace of ~108 mL above the packed soil). The boxes were equipped with a removable top lid, two septa for gas sampling at the back and a removable front plate (Fig. 1). A Luer lock needle was inserted into each septum as a vent for the headspace. For gas tightness, rubber seals were installed between the removable parts and the main body of the incubation boxes. In addition, desiccator grease was applied to the joints. A comparable set-up for imaging trace metals and O_2 in a marine sediment without gas sampling has been described by Stahl et al. (2012).

The planar oxygen optode-sensing layer was directly coated onto the removable front plates. For P and trace metal sampling, DGT gels were taped onto the optode layer. A polycarbonate filter membrane (Nuclepore, 0.4 μm pore size, 10 μm thickness) covered the front of the incubation boxes (at the interface with the removable front plate), ensuring a stabile soil profile (see Section 2.3) when the boxes were opened, as well as preventing particle contamination of the DGT gels or physical damage to the optode.

2.3. Box filling

The soil profiles in the six boxes were prepared layer by layer. Pre-incubated bulk soil was put in the boxes first and carefully tamped for even distribution and compaction. The amendment layer was added on top of the bottom bulk soil layer. An amount, equal to 3.4 mg P, of both amendments (solids and char) was freshly, homogeneously mixed into the bulk soil, resulting in a P addition of 94 mg kg^{-1} soil in the amendment layer soil. After adding another portion of unamended bulk soil on top of the amendment layer, the box was tamped again several times. This gentle compaction resulted in an evenly distributed, well-aerated soil profile with a bulk density of 1.3 g cm^{-3} and a total height of 5.5 cm with the treatment layer approximately 1.0 cm thick located in the middle (± approx. 2 mm) of the profile (Fig. 1). For the control treatment boxes, a layer of unamended bulk soil, similar to the bottom and top layer, was packed into the middle part of the soil profile instead. In order to reach the desired water content, corresponding to a soil water potential of −10 kPa (pF 2.0, soil water content of 19.4 wt%), MilliQ-water (prepared by a Millipore Elix S, electrical resistance: 18.2 MΩ cm^{-1}) was added dropwise to the top of the packed soil.

Table 1
The chemical properties of the soil amendments: dry manure solids and derived char. n.d.: not determined.

Properties		Solids	Char
Total N	(mg g^{-1} DM)	28.6	n.d.
Ammonium-N	(mg g^{-1} DM)	18.1	n.d.
Total P	(mg g^{-1} DM)	20.4	53.8
Total K	(mg g^{-1} DM)	9.2	24.3
Total Ca	(mg g^{-1} DM)	19.9	57.1
Total Fe	(mg g^{-1} DM)	1.3	4.2
Total Al	(mg g^{-1} DM)	0.7	1.8
Volatile solids	(% w/w)	84.3	58.6
Ash	(% w/w)	15.7	41.4

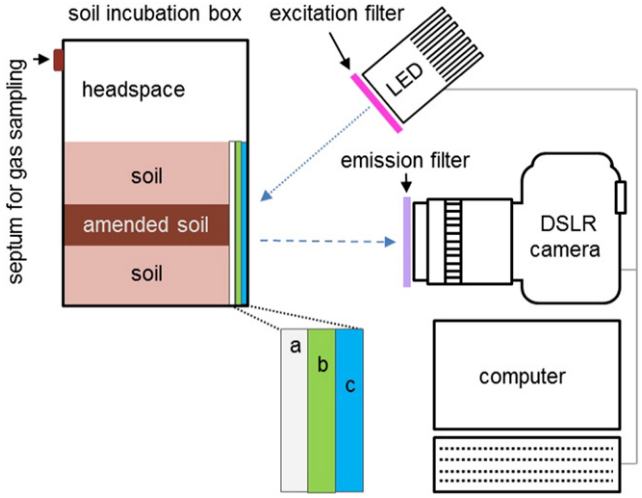

Fig. 1. Schematic overview of the experimental setup (not to scale). Excitation filter: 470 nm short-pass filter; emission filter: 530 nm long-pass filter. (a) filter membrane, ~10 μm thick, (b) DGT gel, ~100 μm thick, and (c) planar optode, ~30 μm thick.

2.4. Incubation experiment

The filled experimental boxes were incubated in darkness at room temperature (19.5 ± 0.5 °C) for 23 days. The gravimetrically determined water loss due to evaporation was compensated for by regular addition of MilliQ-water throughout the experiment. Three of the six incubation boxes were placed next to one another, while the remaining three were stacked on top of the bottom row.

2.4.1. Oxygen imaging

Planar optode images, covering all six incubation boxes in one image, were taken every 30 min, starting within the first 3 h after experimental setup until day 7. Afterwards the imaging interval was lengthened to every 2 h for the following 16 days. Minor changes to these intervals were necessary to allow for DGT gel application and removal. The images were processed using the free software ImageJ (http://rsbweb.nih.gov/ij/).

2.4.2. DGT sampling

DGT gels were deployed for 24 h following five different incubation periods: 0 h (immediately after setup), 24 h, 168 h (one week), 336 h (two weeks) and 504 h (three weeks) after experimental setup. At each application time the front plates were removed and one DGT strip was mounted vertically onto each plate between the protective membrane and the planar oxygen optode using adhesive tape (Scotch Super 33 + Vinyl Electrical Tape, 3M, USA). In this spatially resolved DGT application we replaced the standard, 0.8 mm thick diffusive gel by a 0.01 mm thick membrane in order to reduce image blurring through lateral solute diffusion to a minimum (Santner et al., 2015a, 2015b). This changed DGT geometry leads to increased DGT mass uptake compared to the standard geometry, however provides a significantly more accurate representation of the spatial solute distribution. The soil water content was not increased prior to DGT application as is often done in bulk soil DGT experiments, as the water content was generally high. The location of the DGT gel was shifted horizontally across the packed soil body at each application. After gel retrieval, the gels were dried and prepared for LA-ICP-MS analysis.

2.4.3. GHG sampling

Gas samples were taken manually throughout the incubation period, starting immediately after the first DGT application (within 3 h of the start of the experiment). The sampling frequency was chosen according to the expected GHG emission pattern and potential disturbances: shorter sampling intervals in the initial experimental phase and in connection with box openings (due to DGT gel deployment or removal).

2.5. Measurement of oxygen profiles using planar optodes

The measuring principle of planar oxygen optodes has previously been described in detail (Larsen et al., 2011). Briefly, the O_2-quenchable luminophore Pt(II)-tetrakis(pentafluorophenyl)porphyrin (PtTFPP), was combined with an antenna dye (the coumarin dye Macrolex® fluorescent yellow 10GN) to increase the brightness of the fluorescent signal. The platinum (II) complex and the antenna dye were dissolved in a 4 wt% polystyrene matrix, using chloroform as the solvent, and were then directly coated onto 2-mm thick glass inserts using a small airbrush. The glass inserts (50 × 50 mm) were fitted into the front window of the incubation boxes. The excitation light was supplied by seven blue light-emitting diodes (λ-peak = 447.5 nm; Luxeonstar, SR-02-R0500, Canada) equipped with a short-pass filter (475 nm; TECHSPEC, USA). Images of the fluorescent light emitted by the optode were captured by a modified digital single-lens reflex camera (Canon EOS 1100D), equipped with a macro lens (Sigma 50 mm F2.8 EX DG Macro) and a long-pass emission filter (OG 530, Schott, Germany) to remove any reflected excitation light. The camera chip can acquire 4272 × 2848 pixels, which, at the given optical configuration and with a pixel binning of 2 × 2, cover an effective area of 27.9 × 18.6 cm, providing a spatial resolution of 130 × 130 μm pixel^{-1}.

The principles of the optode calibration procedure applied in this study have been described in Larsen et al. (2011). In order to mimic the experimental conditions, a strip of DGT gel (1 cm × 5 cm) was mounted on the optode during the calibration procedure. Optode calibration was carried out in the incubation boxes, which were filled with MilliQ-water at ambient conditions (19.5 ± 0.5 °C). The MilliQ-water was purged with N_2 (AGA, Laseroxygen 3.5, 99.99% purity) for 4 h prior to use. The O_2 level in the N_2-purged water was increased stepwise by purging with ambient air and then monitored continuously using an O_2 meter (HI9146, HANNA instrument, USA). Six O_2 levels (0, 17, 40, 55, 70 and 100%) were used to make the calibration curves. As with most other O_2 optode sensors, a modified Stern-Volmer equation adequately described the response of the setup in this study (Eq. 1) (Klimant et al., 1995):

$$\frac{R}{R_0} = \alpha + (1-\alpha)\left(\frac{1}{1+K\cdot C}\right) \quad (1)$$

where α is the non-quenchable fraction of the luminescence signal, K is the Stern-Volmer quenching constant, R is the (red-green)/green luminescent intensity ratio, R_0 is the ratio in the absence of O_2, and C is the dissolved O_2 concentration. The average K and α values of the sensor in each optode box were determined by individual calibration curves.

2.6. Greenhouse gas measurement

Two septa, each inserted with a needle, were embedded in the back of each incubation box. Before gas sampling, the headspaces of the incubation boxes were flushed with ~100 mL ambient air through one of the septa, while the second needle was opened to serve as a vent. After flushing, the venting needle was closed with a customised septum lid, and a 5 mL polypropylene syringe was inserted through the other septum, which was then filled from and emptied into the headspace three times to mix the headspace gas. Subsequently, a gas sample (5 mL) was taken from the headspace and transferred to 3-mL vacuum vials (Labco, UK). The first 3 mL of the sample were flushed into the vial, while the remaining 2 mL were added to the vials as overpressure. For each incubation box and sampling time, three samples were taken 0, 10 and 20 min after headspace flushing, repeating the gas mixing for each of these three samplings. After gas sampling, the two needles were opened again to maintain the air circulation between the ambient air and the headspace in the box.

Gas emission rates were estimated from the increase in concentrations of the respective gases in the box headspace, assuming a linear increase in concentrations during the 20-minute sampling time. This assumption was verified in a preliminary experiment by measuring gas concentration increases for 40 min with a 10-minute interval using the same set-up.

All the gas samples were analysed for concentrations of nitrous oxide (N_2O), carbon dioxide (CO_2) and methane (CH_4) by gas chromatography using a Greenhouse Gas Analyser (450-GC, Bruker, Germany), which is configured with two chromatographic channels: an electron capture detector (ECD) channel (Hayesep N pre-column (0.5 m), Hayesep D column (2.0 m), temperatures: oven 50 °C and detector 200 °C, carrier gas: argon with 5% methane) for N_2O analysis, and a thermal couple detector/flame ionisation detector (TCD/FID) channel (Hayesep N pre-column; Porapak QS column (2.0 m); detector temperatures: TCD: 350 °C, FID: 300 °C; carrier gas: helium) for CO_2 and CH_4 analysis.

2.7. Analysis of 1D profiles of phosphorus and trace metal availability

A DGT resin gel with anion and cation-binding capacity was used for the spatially-resolved sampling of phosphate and trace metal cations across the profile of the soil packed into the incubation boxes. The high-resolution mixed binding gel (HR-MBG), developed for chemical imaging based on laser ablation-inductively coupled plasma-mass spectrometry (LA-ICP-MS), contains zirconium-hydroxide as the anion resin and suspended particulate reagent-iminodiacetate as the cation resin material embedded in an ether-based urethane polymer hydrogel (Kreuzeder et al., 2013). Sheets of the HR-MBG were produced and kept refrigerated at 6 °C in a storage solution containing 10 mmol L^{-1} $NaNO_3$ until experimentation.

Calibration standards were made by putting HR-MBG discs in commercially available DGT holders (DGT Research, Lancaster, UK) with a defined opening area, which were immersed in solutions containing different amounts of phosphate and trace metal cations (Mn, Ni, Cu, Zn, Cd and Pb) at ambient temperature for 24 h in four replicates. The analyte loading of the gel discs was determined by digestion of three of the replicates after retrieval from the DGT samplers. The fourth gel disc replicate was dried and used as the calibration standard during LA-ICP-MS (Kreuzeder et al., 2013).

For application of the DGT gel to the soil profiles, the sheets of HR-MBG were cut into strips approximately 6 × 1 cm and also stored at 6 °C in 10 mmol L^{-1} $NaNO_3$ until application.

For DGT deployment in the incubation boxes, the boxes were carefully opened and the HR-MBG strips were applied vertically over the whole soil profile to the removable, optode coated, perspex plate. After gel mounting the boxes were closed. See Section 2.4 for details.

After retrieval from the incubation boxes, the HR-MBG strips were put on a polyethersulfone membrane (Supor 0.45 μm, Pall, USA) and dried in a gel dryer (GIBCO GD 40/50, Life Technologies, Gaithersburg, MD, USA). This procedure dries the DGT gels while keeping them dimensionally stable. After drying, the gel and membrane were inseparable from one other. The gel and membrane assembly was then mounted on a glass plate using double-sided adhesive tape.

LA-ICP-MS analysis was performed on a quadrupole ICP-MS instrument (NexION 300D, Perkin Elmer, USA) coupled to an excimer laser ablation system (UP 193-FX, ESI, NWR Division, USA). For each sample strip, five parallel ablation lines with 1 mm distance between the lines were measured. The ablation system was set to an energy output of 0.15 J cm^{-2}, 30 Hz laser pulse frequency, 150 μm laser spot size and

200 μm s^{-1} scan speed. The following isotopes were analysed: ^{31}P, ^{55}Mn, ^{60}Ni, ^{63}Cu, ^{66}Zn, ^{111}Cd and ^{208}Pb. Additionally, ^{13}C was measured and used as an internal normalisation standard.

In order to compensate for the small-scale (sub-mm) variability of the P distribution, the average of five ICP-MS readings along the analysed profiles and across the five parallel lines for the two replicate treatments was taken, resulting in one final data point being the average of 50 ICP-MS readings. The final spatial resolution of the analyte profiles was therefore approximately 1.1 mm. The blank level for P on the DGT gel was ~0.02 μg cm^{-2} with a common signal variability in the LA-ICP-MS analysis of ~25% (Kreuzeder et al., 2015). The blank was corrected for by subtraction.

2.8. Bulk soil analysis

One day after the final DGT gel application, the soil in the boxes was destructively sampled. Each packed profile was cut horizontally into five slices approximately 1.1 cm thick. The soil slices were mixed thoroughly. The water content of these samples was measured by drying at 105 °C for 24 h. Furthermore, the samples were extracted with 0.05 mol L^{-1} calcium nitrate solution ($Ca(NO_3)_2 \cdot 4H_2O$, puriss p.a., Sigma Aldrich) at a soil:solution ratio of 1:5 (modified after McLaren et al. (2007)). Three replicate aliquots (5 g dry matter equivalent) from each soil layer were weighed into 50 mL centrifuge tubes (Polypropylene Cellstar® tubes, Greiner Bio-One, Germany). Twenty-five milliliters of 0.05 mol L^{-1} $Ca(NO_3)_2$ solution was added to the tubes, which were closed and put into an end-over-end shaker for 2 h at 35 rpm. The extracts were then centrifuged at room temperature for 5 min at 1000 rpm (Eppendorf Centrifuge 5810R, Germany). Afterwards, the supernatant was filtered (Whatman filter papers 44, GE Healthcare, UK) into sample vials. For P analysis, the extracts were kept refrigerated until analysis. For ICP-MS analysis of the trace metals (Mn, Ni, Cu, Zn, Cd and Pb), the filtered extracts were acidified to 2% HNO_3 and stored at room temperature. Samples from the experimental start (stored in the meantime at −18 °C) were processed in the same way. Additionally, the freshly mixed pre-incubated soils with amendments (manure solids and char respectively) were analysed. After filtration, the pH (PHM210 MeterLab® Radiometer Analytical, France) was measured in the remaining unfiltered extract.

The soil extracts were analysed for molybdate-reactive phosphate on a Flow Injection Analyser (FIAstar 5000, FOSS, Denmark). A modified colour reaction using tin(II)-chloride as the reductant and measurement of absorbance at 720 nm was used (Murphy and Riley, 1962).

For ICP-MS (NexION 300D, Perkin Elmer, USA) analysis of the soil extracts, ^{115}In was used as the internal normalisation standard. All samples, calibration standards and in-house quality controls were matched to a 2% HNO_3, 0.05 mol L^{-1} $Ca(NO_3)_2$ matrix.

2.9. Statistical analysis

Analysis of Variance was used to determine the significance of differences in measured variables between treatments. Data distribution normality was verified using the Shapiro-Wilk test. Statistical differences, for which $p < 0.05$, are referred to in the text as significant.

3. Results

3.1. Oxygen dynamics in soil

Different patterns in O_2 concentration were observed in the amended soils compared to the control (Fig. 2), as were effects caused by opening the box and gas sampling events.

The initial ($t = 0$) average O_2 levels in the control and char treatments (93% and 91% air saturation respectively) were significantly higher than that in the manure solids treatment (78% air saturation). The O_2 levels in the soil with the solids layer were consistently lower throughout the entire experimental period than in the control and char layer-amended soil (Fig. 2). The char-amended soil had a slightly lower O_2 level than the control, but this difference was not statistically significant (Mann-Whitney Rank Sum test, $\alpha \leq 0.05$). Even though the gas sampling events caused an increase in O_2 for all treatments, the O_2 levels reached their respective consistently decreasing O_2 levels again within 2 to 4 h of the experimental boxes being closed. Opening the boxes for DGT gel application led to even more extensive increases of O_2 in all treatments. Nevertheless, after 4 to 6 h, the O_2 concentration had reached approximately the same level as prior to the DGT application.

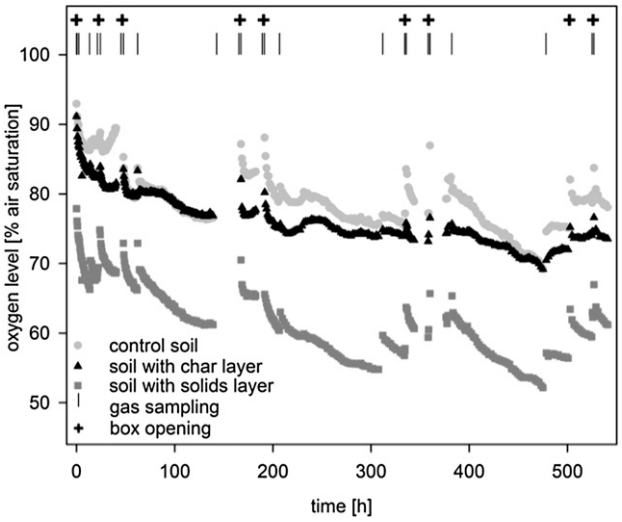

Fig. 2. Average O_2 levels in soil during the experimental period, obtained from the optode images covering a 5 × 5 cm soil area. Each data point represents the mean of two replicates. Error bars are not shown to maintain clarity, but can be found in an equivalent figure in Supplementary material (Fig. S1).

Generally, this data showed a decrease in O_2 levels in all the soil treatments and the control over time (Fig. 2). The average O_2 levels decreased to the greatest extent within the first week, during which they declined by 16%, 14% and 17% air saturation in the control, char-amended and manure solids-amended soil respectively. After three weeks, the O_2 level had dropped by 23%, 22% and 26% air saturation in control, char-amended and manure solids-amended soil respectively.

The vertical profile of O_2 contents indicated a more or less uniform distribution of O_2 along the profile (Fig. 3), particularly in the solids-amended soil. Although differences in the O_2 levels between treatments were observed, no differences in O_2 were observed between the amended soil layer and the over- and underlying unamended layers within the treatments.

3.2. Gas emissions

3.2.1. Carbon dioxide

The CO_2 emissions were highly dependent on the amendments to the soil (Fig. 4). Soil amended with a manure solids layer consistently emitted more CO_2 than the control soil and the soil with the char layer. This difference gradually increased throughout the experimental period. The CO_2 emission from the char-amended soil was not significantly different from that of the control during the first nine days (207 h). Nevertheless, after the full experimental period, the cumulative CO_2 emissions from the soil with the char layer were 245 μg CO_2-C kg^{-1} soil lower than that of the unamended control soil (355 μg CO_2-C kg^{-1} soil), which was found to be a significant difference.

Accordingly, the highest CO_2 emission rates (the slope of the curves in Fig. 4) were observed in the manure solids layer (3–4 μg CO_2-C kg^{-1} soil h^{-1}), whereas very low CO_2-emission rates (<1 μg CO_2-C kg^{-1} soil h^{-1}) were found from the soil with the char-amended

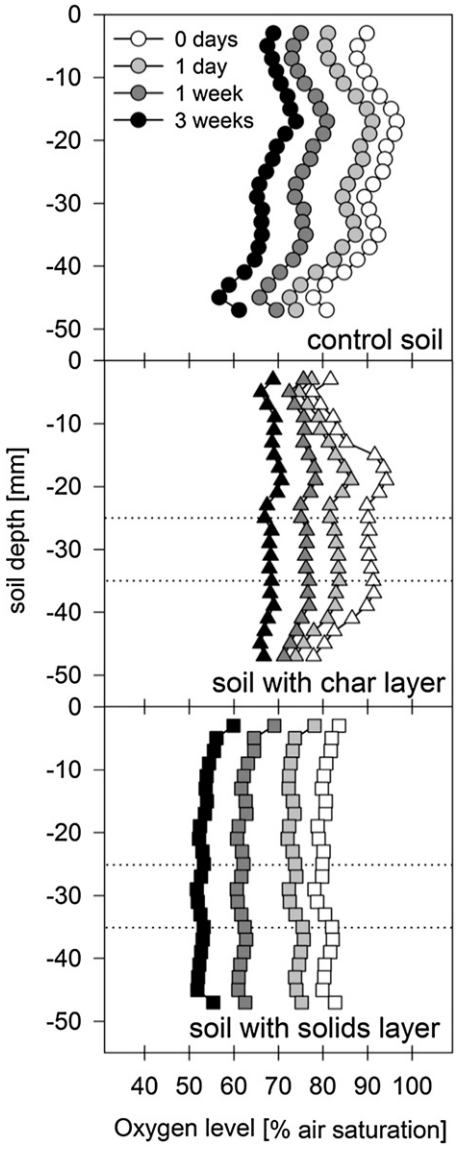

Fig. 3. Oxygen levels covering 0.2-cm-high and 5 cm-wide horizontal bands through the soil profile. Data of 1 day, 1 week and 3 weeks were measured just before the incubation box opening events. The approximate position of the char-amended or solids-amended layer is indicated by the dotted lines. Each data point represents the mean of two replicates. Error bars are not shown to maintain clarity, but can be found in an equivalent figure in Supplementary material (Fig. S2).

layer, with control CO_2-C emission rates being slightly higher than those of the soil with the char-amended layer.

3.2.2. Nitrous oxide and methane emissions

N_2O and CH_4 emissions were generally very low and no significant treatment effect was observed (data not shown). For N_2O emissions, none of the treatments exceeded the rate of 0.6 μg N_2O-N kg^{-1} soil h^{-1} at any time during the experiment. Nevertheless, there was a tendency for the soil with the manure solids layer to emit slightly more N_2O in the initial phase of the incubation (first 24 h). After day 1, however, the emission rate of the manure solids-amended soil decreased and was within the same range as that of the control. As observed for CO_2, the soil with the char-amended layer showed slightly lower N_2O emissions than the control. No such general pattern over time for any treatment was observed for CH_4 emissions, which were close to zero in all treatments.

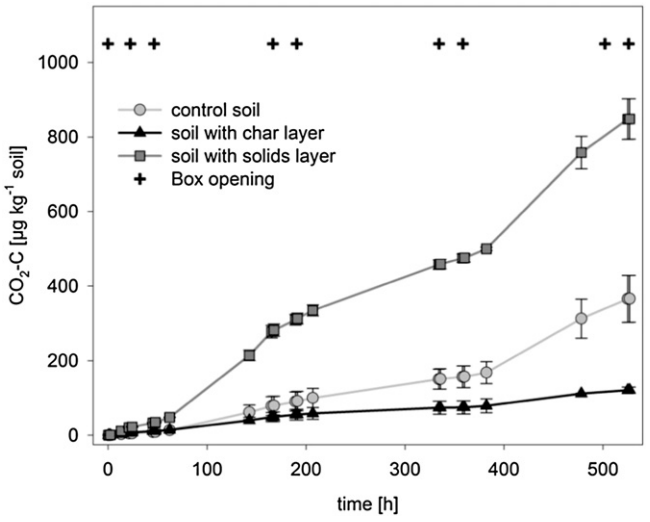

Fig. 4. Cumulative CO_2 emissions from soil, as influenced by the amendments. The cumulative emissions were calculated using linear interpolation across sampling intervals. Each data point represents the total emission from the initial to the sampling time point. Error bars represent standard error of the mean ($n = 2$).

3.3. P and trace metal availability in the soil

3.3.1. 1D profiles of DGT-labile P

With respect to the P distribution measured on DGT gels, there was a treatment, layer and time effect (Fig. 5). For the control soils, there was a slight increase in DGT-labile P with increasing soil depth. From the top to bottom of the soil profile, the surface concentration of P on the DGT gel increased by approximately 0.10 μg cm^{-2}. Generally, the DGT-labile P in the control DGT gels was very low, since the P content in blank gels, which had not been in contact with soil at any stage, varied between 0.10 and 0.21 μg P cm^{-2}.

The char-amended and manure solids-amended soil layers showed considerably higher DGT-labile P over the whole incubation period. For the manure solids-amended layer, the DGT-labile P decreased over time. The highest values were observed during the early application periods (0–24 and 24–48 h), but afterwards DGT-labile P decreased over time. The development of DGT-labile P in the char-amended layer showed a contrasting pattern. After varying, but relatively low amounts of DGT-labile P in the first weeks of the experiment, the amount increased after three weeks of incubation. At the end of the experiment, the amount of DGT-labile P seemed very similar in the char-amended and manure solids-amended soils.

By integrating the DGT-labile P in the peak area (Fig. 6B), it could also be shown that there was a general increase in P availability over time from the soil amended with char. Nevertheless, the total amount of DGT-labile P in the soil amended with solids was higher than in the char-amended soil throughout the incubation period. Despite the decrease in absolute DGT-labile P within the solids-amended soil layer over the three weeks, the P peak width increased to a greater extent than after char addition (Fig. 6A), resulting in a larger total amount of DGT-labile P within the peak area. From week 1 to week 3, there was a tendency for the gel P content to be slightly higher in an approximately 5 mm-wide soil layer just below the solids-amended treatment layer. In the soil above the treatment layer, however, no clear difference in DGT-labile P compared with the control soil was observed.

3.3.2. DGT loading with other elements

DGT-labile metals did not show a layer, treatment or time effect. However, DGT-labile Cu, Ni and Zn increased with increasing soil depth although the char and manure solids amendments did not result in an increase in the DGT-labile fraction. DGT-labile Mn, Cd and Pb

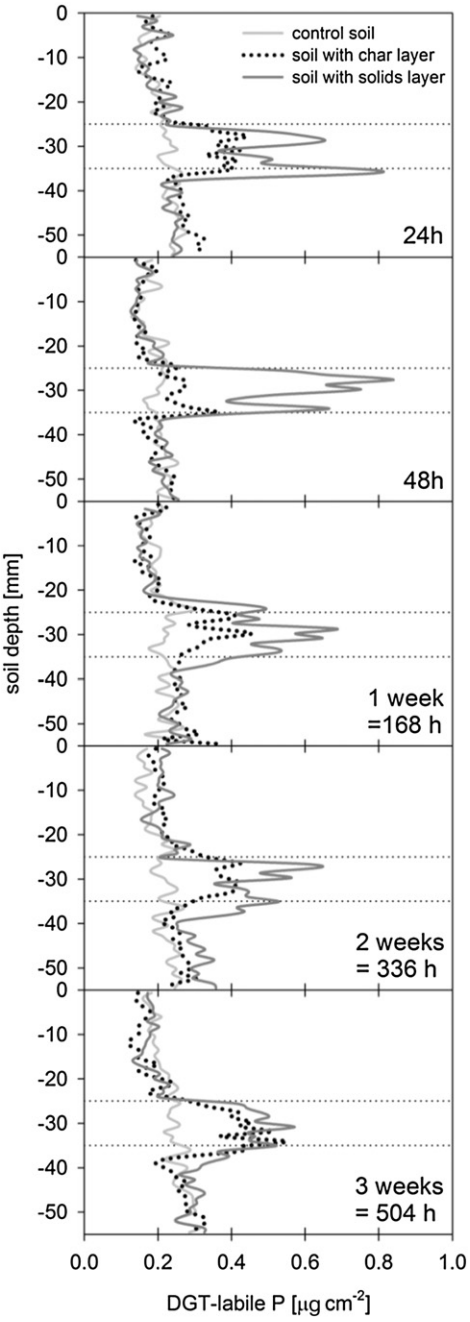

Fig. 5. Average depth profiles ($n = 50$) of DGT-labile P for the control treatment and soils with the char or manure solids layer (position indicated by the dotted horizontal lines) for the five DGT application times.

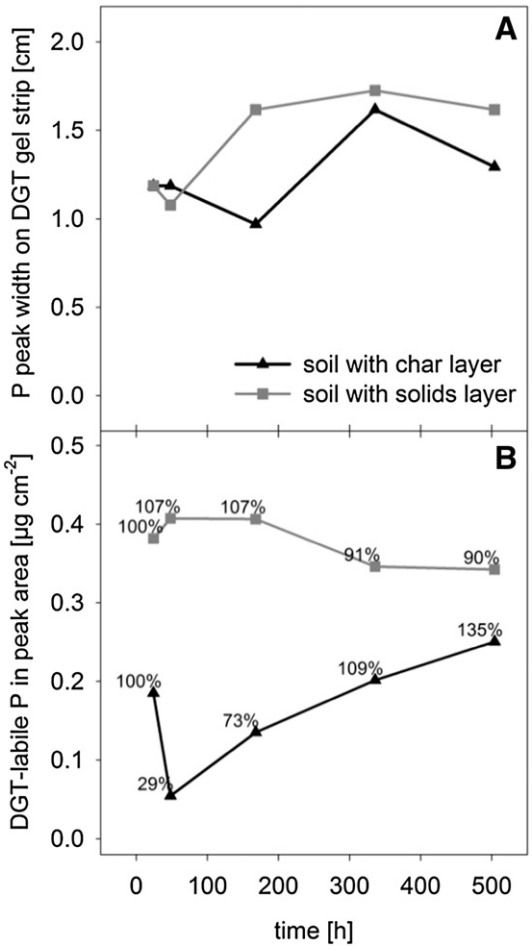

Fig. 6. (A) Width of the zone of increased P availability as measured by DGT and (B) amount of DGT-labile P in the amended soil layers during the experimental period. The amounts of P were obtained by integrating the DGT-measured peaks of labile P (see Fig. 5). To allow for easier comparison of the relative changes over time within the treatments, DGT-labile P in the peak area is displayed as percentage of the value obtained after 24 h for the char and manure solids treatments, respectively. Each data point represents the mean of two replicates.

showed no difference across the soil profile in any of the treatments (data not shown).

3.3.3. $Ca(NO_3)_2$ extractable P

Extractable P differed significantly between treatments and between amended and unamended soil layers. Moreover, differential temporal trends could be observed for manure solids-amended and char-amended soil layers.

Directly after initiation of the soil incubation (day 0), extractable P was several times higher in the manure solids-amended soil than in the significantly lower char-amended soil and the control soil (Table 2).

After 23 days of incubation, extractable P in the manure solids layer had decreased significantly by 87%, while it roughly doubled in the char layer. Nevertheless, significantly more P was extractable from the manure solids-amended soil than from the char-amended soil after 23 days. Extractable P did not change relevantly in the control soil during the incubation period, always being significantly lower than the amended soil layers. The soil layers directly adjacent to the amended soil layers showed increased extractable P at the end of the incubation period.

3.3.4. Other elements in the $Ca(NO_3)_2$ soil extracts

In agreement with the DGT-LA-ICP-MS data, no treatment or layer effect was observed for any of the other elements (Mn, Ni, Cu, Zn, Cd or Pb; data not shown). The elemental concentrations were generally low and partly below detection limits.

3.4. Soil pH and water content

The pH was stable throughout the experiment in all treatments (±0.1 pH units). Nevertheless, the char-amended treatment layer had a slightly higher pH than the unamended bulk soil or the manure solids-amended treatment layer (Table 2).

After 23 days of incubation, increasing water content with increasing soil depth was observed (Table 2). The bottom soil layer contained approximately 3% more water than the top soil layer. The increase in moisture content at greater soil depth was significant, however no significant difference between the treatments was observed.

Table 2
P concentration and pH in the extracted soil layers at setup (day 0, analysis of the amended and unamended (*) bulk soils before box filling) and at final soil sampling (day 23), as well as the range of soil water content ($n = 2$) in the soil layers at day 23. Grey shading: approximate location of char/manure solids layer. Vertical lines indicate that the value given in the middle layer (22-33 mm) represents the value for the whole soil profile, as there is no amended layer in the control treatment. Standard deviations are given in parentheses ($n = 6$ for pH and P concentration). Values are significantly different if letters are different (Tukey test, $\alpha \leq 0.05$).

Soil depth [mm]	Control soil				Soil with char layer				Soil with manure solids layer			
	Day 0		Day 23		Day 0		Day 23		Day 0		Day 23	
	P concentration [mg P kg^{-1}soil] in 0.05 mol L^{-1} $Ca(NO_3)_2$ extract											
0 – 11	|	|	0.27 [a]	(0.01)			0.29 [a]	(0.01)			0.28 [a]	(0.01)
11 – 22	|	|	0.28 [a]	(<0.01)			0.40 [b]	(0.04)			0.48 [b]	(0.05)
22 – 33	0.25*	(<0.01)	0.28 [a]	(0.01)	0.83 [c]	(0.03)	1.58 [d]	(0.15)	15.50 [f]	(1.70)	2.09 [e]	(0.07)
33 – 44	|	|	0.28 [a]	(0.01)			0.42 [b]	(0.05)			0.49 [b]	(0.05)
44 – 55	|	|	0.27 [a]	(0.01)			0.29 [a]	(0.01)			0.29 [a]	(0.02)
	pH (in 0.05 mol L^{-1} Ca $(NO_3)_2$ extract)											
0 – 11	|	|	6.73	(0.02)			6.70	(0.04)			6.70	(0.03)
11 – 22	|	|	6.72	(0.02)			6.71	(0.01)			6.72	(0.03)
22 – 33	6.59*	(0.03)	6.72	(0.02)	6.68	(0.00)	6.78	(0.02)	6.63	(0.01)	6.73	(0.01)
33 – 44	|	|	6.71	(0.03)			6.72	(0.02)			6.73	(0.01)
44 – 55	|	|	6.73	(0.02)			6.68	(0.02)			6.69	(0.01)
	Soil water content, min. & max. [%]											
0 – 11			18.2	18.3			18.2	18.6			18.0	18.1
11 – 22			18.6	18.9			18.5	18.9			18.0	18.6
22 – 33			19.0	19.2			19.6	19.7			19.1	19.7
33 – 44			20.0	20.1			20.1	20.3			20.3	20.4
44 – 55			21.2	21.6			21.4	21.7			21.1	21.6

4. Discussion

4.1. Oxygen dynamics affected by the amendment of manure solids and char

The O_2 levels in soil amended with manure solids and char decreased over time, but contrary to this study's hypothesis, no localised O_2 depletion in the soil layer amended with manure solids or char was observed. The water content of the soil was moderate, with an air-filled pore space as high as 35%, allowing for relatively fast diffusion of O_2 from the headspace to the soil. Accordingly, no depletion zones around the residuesphere were observed, but the overall O_2 consumption in the soil with the manure-solids amended layer was much higher, due to the greater availability of organic C for microbial turnover. Nitrification, which consumes two moles of O_2 per mole of oxidised ammonium, could also have contributed to the higher O_2 consumption (Small et al., 2013).

In addition, the soil O_2 dynamics are closely linked to the soil redox potential (Cook et al., 2013), which can be indicated effectively by temporal and spatial changes in the availability of Mn, which is highly redox sensitive (Mundus et al., 2011). However, no differences in Mn availability were found between soil layers or even between treatments during this experiment, therefore reductive (co-) dissolution of solutes can be excluded from contributing to P mobilisation in this study.

The general pattern of O_2 dynamics throughout the incubation period was not affected by box opening and the concurrent introduction of ambient air. The boxes were opened for approximately 1–2 min, either to apply or remove the DGT gels. This opening event introduced ambient O_2 to the soil profile (Fig. 2), but the O_2 levels in the soils rapidly dropped to their value prior to the opening.

With a rather small volume of headspace (108 mL) in the incubation boxes, gas sampling resulted in a pressure change in the headspace, consequently boosting gas diffusion or transport into the soil profile and therefore increasing soil O_2 levels. This perturbance was short-lived and faded within a few minutes of the gas sampling being completed.

4.2. GHG emissions

As expected, the highest CO_2 emissions were observed for the manure solids-amended soil, which was reasonable because this material contained more degradable C than the char (Zhu et al., 2014). Much lower CO_2 emissions from the char-treated soil (compared with the control) indicated not only lower C mineralisation from the char, but

even an inhibition of native soil organic matter degradation. This result is in line with the study by Spokas et al. (2009) where biochar amendments also suppressed CO_2 production compared with the control soil. Generally, char produced at a high temperature (>500 °C) shows low C mineralisation in soil as compared to chars produced at lower temperatures (Zimmerman et al., 2011; Bruun et al., 2014). Moreover, char has been shown to strongly sorb natural organic matter (Cornelissen et al., 2005; Sobek et al., 2009), possibly reducing the availability of dissolved soil organic matter for decomposition. Other additional mechanisms may also contribute to the char-induced reduction of CO_2 emissions, such as changes in ionic strength resulting in deactivation or activity suppression of microbial enzymes (Quiquampoix and Burns, 2007).

The average O_2 levels in all treatments never fell below 50% air saturation. Under these conditions, denitrification and methanogenesis do not occur, therefore CH_4 emissions were close to zero during the entire experiment. Without any anoxic conditions occurring, even around the amendment-mixed soil layer, denitrification was unlikely to be observed. Furthermore, oxic conditions with more than 50% air saturation of O_2 contents favoured complete nitrification with fewer by-products (Khalil et al., 2004). Consequently, N_2O production from either denitrification or nitrification was very low.

4.3. Temporal and spatial changes in the availability of P and metals

4.3.1. P availability

DGT-measured parameters have repeatedly been shown to be good indicators of plant P availability, often superior to standard soil (P) tests (Tandy et al., 2011; Six et al., 2013; Mason et al., 2013). Recently, DGT has also been shown to be suitable as a means of testing P availability from organic soil amendments (Six et al., 2014).

There was a contrast in the temporal changes in P availability between manure solids and char: whereas the initial P availability from manure solids was high but decreased slightly over time, the P availability from char showed an increase during the three week-incubation period. After the three-week incubation, the DGT-labile P in the char-amended soil layer was still considerably lower compared to the solids treatment though (Fig. 6). These observed temporal patterns for the solids and char were in agreement with earlier studies by Christel et al. (2014) and Christel et al. (in press); the decrease in P availability from the manure solids is most likely due to either adsorption or immobilisation into microbial biomass of the easily available P pool abundant in the solids. Similarly, Peirce et al. (2013) found that manure P availability declined with storage time. However, for the char the gradual increase in P availability is more likely to be caused by dissolution reactions from the calcium-phosphate forms most probably present in the char (see Table 1 elemental composition) for which the slightly acidic pH would favour dissolution. In the present study and the cited studies, the total amount of DGT-labile P supplied to the soil from the solids was higher than from the char, suggesting a greater potential of solids being applied as P fertiliser. Taking the peak width over time into account, char appears to remain a very local source of P, even more so than the solids. This highlights the importance of securing close proximity between the applied manure-derived fertiliser and plant roots.

The significantly higher CO_2 emissions and greater O_2 consumption in the solids-amended treatment compared to the char-amended and control treatments indicated that uptake of P by microbes might have played a role in decreasing P availability in this treatment. However the main P immobilisation process was most likely sorption of phosphate to Fe- and Al-(oxy)hydroxides in this carbonate-free soil. The much smaller decrease of DGT-labile P compared to $Ca(NO_3)_2$-extractable P after 23 days soil incubation provided good evidence for sorption being the main P immobilisation process, as DGT samples reversibly adsorbed P, which is often not equally accessible to weak salt extracts (Santner et al., 2015b). As respiration in the char-amended soil was very low, the increase in P availability over time was likely to be governed by abiotic processes. Phosphate adsorbed to the surface of the char (Laird et al., 2010) might have been desorbed. Moreover, the continuous removal of phosphate from the soil solution by the DGT gel might have induced dissolution of phosphate minerals, which precipitated on the surface of the char during pyrolysis. Information about P speciation in pyrolised pig manure solids is very limited, but P-containing precipitates such as amorphous Ca-phosphates and nano-crystalline phosphate precipitates have been identified in pyrolised broiler litter (Uchimiya and Hiradate, 2014). Since no distinct O_2 depletion within the amendment layer was observed and the soil water content was equivalent to pF 2, a redox-induced remobilisation of soil-borne P (Grunth et al., 2008) was not expected to contribute to increased P availability within the amendment layer.

Regarding spatial changes in P availability, no increase in the soil directly adjacent to the char-amended soil layer was observed, highlighting the very limited mobility of the DGT-labile P in the soil solution. For the amendment of the manure solids, there was a slight increase in P availability in the soil below the amendment layer, which could be related to the mass flow of P-containing manure particles with vertical water movement, as diffusive transport should also be visible at the upper edge of the amended layer. However, due to uncertainty about the precise location of the amendment layer (of approx. ±2 mm), this observation requires further investigation to be confirmed.

At final soil sampling it was not possible to sample the amendment layer distinctly from the adjacent amendment-free soil layers. The slight increase in $Ca(NO_3)_2$-extractable P in the soil layers adjacent to the amendment layer was therefore most likely caused by small contaminations with char or manure solids from the amendment layer. Nevertheless, the observation of manure solids and char amendments both remaining a localised P source over the whole incubation period emphasised the importance of fertiliser placement in relation to roots for optimal P uptake by plants. At the same time, no risk of P leaching to groundwater reservoirs would be expected after application of these materials to a P-depleted soil.

The general increase in DGT-labile P in the lower part of the soil profiles could be linked to increased P diffusivity within the soil due to a better connectivity of water-filled pores. Increasing DGT availability of P and trace metals due to increased soil water content has previously been reported (Hooda et al., 1999; Menzies et al., 2005).

4.3.2. Availability of other elements

The fact that no increases in the availability of any of the other elements, including critical heavy metals contaminants such as Cu, Cd and Zn, were detected in this study suggested that there was no issue with increased metal loads in the amended soils. Compared to typical soil background contents, the total amount of Cu, Cd and Zn added was negligible.

4.4. Perspectives for future studies

As this study was a first attempt to investigate GHG emissions in combination with a sandwich optode/DGT sensor in a soil environment, some methodological challenges were encountered that should be considered for future studies. It is important to prevent artefacts in both the O_2 and the GHG measurements being introduced by the opening of the incubation boxes for DGT gel application and removal. One option could be to open them in a controlled atmosphere, e.g. a glove box, where the O_2 saturation is adjusted to that present at that time in the soil profile. Another option would be to avoid pressure changes in the headspace during gas sampling by installing a pressure change eluviation system, as developed by Zhu et al. (2015). For the exact localisation of the amendment layer, tracer substances that are present in the soil additive, but not in the soil itself, could be used as reference substances for more precise localisation of the treatment layer. Despite these methodological issues, the combination of optode, DGT and GHG emission measurements is a promising tool for simultaneously investigating the spatial

and temporal heterogeneity of O_2 and solute dynamics in a soil system after localised amendment of the soil.

5. Conclusions

Manure solids-C was more degradable than char-C and therefore resulted in increased O_2 consumption in the manure solids-amended soil. Concurrently, more CO_2 was released from the manure solids-amended soil than from the control or the char-amended soil. However, formation of a distinct, O_2-depleted layer did not occur because the entire soil profile was well aerated. Due to a relatively high O_2 content in all treatments, no formation of N_2O and CH_4 occurred in the soil.

The amendment of pig manure solids and that of the derived biochar both increased P availability in the amended soil layer during the three-week incubation, while showing contrasting trends over time. The slower, but increasing temporal pattern of P solubilisation from char was most likely caused by the dissolution of phosphate minerals formed during pyrolysis, while adsorption of soluble P from the manure solids to soil probably governed the decreasing trend of P availability in the solids-amended soil. As microbial activity in the manure solids-amended soil was much higher, which was indicated by the much higher CO_2 emissions, the decrease in P availability might also partly be associated with net P immobilisation in the soil microbial biomass. No distinct differences in P availability in soil after amendment with either manure solids or char could be detected after three weeks. With regard to changes in spatial P availability, both amendments were found to remain a very local P source, not affecting P availability outside the residuesphere.

Consequently in order to use manure solids and char optimally as a P source for plant nutrition, these slow-release P fertilisers should be applied in as close proximity as possible to the developing plant root system, e.g. by controlled injection or placement in relation to the seed.

Acknowledgements

The authors would like to thank Morten Larsen from the Nordic Center for Earth Evolution (Institute of Biology, University of Southern Denmark) for providing the oxygen optodes as well as the technician, Ea J. Larsen, for P analysis of the soil extracts. This study was jointly funded by the CLEANWASTE research project granted by the Danish Council for Strategic Research (2104-09-0056) and the "Climate change: Impacts, Mitigation and Adaptation" PhD scholarship at the University of Copenhagen, as well as by the Austrian Science Fund (FWF): P23798-B16.

Appendix A. Supplementary data

Supplementary data to this article can be found online at http://dx.doi.org/10.1016/j.scitotenv.2016.02.152.

References

Blossfeld, S., Schreiber, C.M., Liebsch, G., Kuhn, A.J., Hinsinger, P., 2013. Quantitative imaging of rhizosphere pH and CO_2 dynamics with planar optodes. Ann. Bot. 112, 267–276.
Bruun, S., Clauson-Kaasa, S., Bobulská, L., Thomsen, I.K., 2014. Carbon dioxide emissions from biochar in soil: role of clay, microorganisms and carbonates. Eur. J. Soil Sci. 65, 52–59.
Christel, W., Bruun, S., Magid, J., Jensen, L.S., 2014. Phosphorus availability from the solid fraction of pig slurry is altered by composting or thermal treatment. Bioresour. Technol. 169, 543–551.
Christel, W., Bruun, S., Magid, J., Kwapinski, W., Jensen, L.S., 2016. Pig slurry acidification, separation technology and thermal conversion affect phosphorus availability in soil amended with the derived solid fractions, chars or ashes. Plant Soil http://dx.doi.org/10.1007/s11104-015-2519-0 (in press).
Cook, F.J., Knight, J.H., Kelliher, F.M., 2013. Modelling oxygen transport in soil with plant root and microbial oxygen consumption: depth of oxygen penetration. Soil Res. 51, 539–553.
Cornelissen, G., Gustafsson, Ö., Bucheli, T.D., Jonker, M.T., Koelmans, A.A., van Noort, P.C., 2005. Extensive sorption of organic compounds to black carbon, coal, and kerogen in sediments and soils: mechanisms and consequences for distribution, bioaccumulation, and biodegradation. Environ. Sci. Technol. 39, 6881–6895.
Davison, W., Zhang, H., 1994. In situ speciation measurements of trace components in natural waters using thin-film gels. Nature 367, 546–548.
Glud, R.N., Ramsing, N.B., Gundersen, J.K., Klimant, I., 1996. Planar optodes: a new tool for fine scale measurements of two-dimensional O-2 distribution in benthic communities. Mar. Ecol. Prog. Ser. 140, 217–226.
Grunth, N.L., Askaer, L., Elberling, B., 2008. Oxygen depletion and phosphorus release following flooding of a cultivated wetland area in Denmark. Danish J. Geogr. 108, 17–25.
Hinsinger, P., 2001. Bioavailability of soil inorganic P in the rhizosphere as affected by root-induced chemical changes: a review. Plant Soil 237, 173–195.
Hjorth, M., Christensen, K.V., Christensen, M.L., Sommer, S.G., 2010. Solid–liquid separation of animal slurry in theory and practice. A review. Agron. Sustain. Dev. 30, 153–180.
Hooda, P.S., Zhang, H., Davison, W., Edwards, A.C., 1999. Measuring bioavailable trace metals by diffusive gradients in thin films (DGT): soil moisture effects on its performance in soils. Eur. J. Soil Sci. 50, 285–294.
Khalil, K., Mary, B., Renault, P., 2004. Nitrous oxide production by nitrification and denitrification in soil aggregates as affected by O_2 concentration. Soil Biol. Biochem. 36, 687–699.
Klimant, I., Meyer, V., Kühl, M., 1995. Fiber-optic oxygen microsensors, a new tool in aquatic biology. Limnol. Oceanogr. 40, 1159–1165.
Kreuzeder, A., Santner, J., Prohaska, T., Wenzel, W.W., 2013. Gel for simultaneous chemical imaging of anionic and cationic solutes using diffusive gradients in thin films. Anal. Chem. 85, 12028–12036.
Kreuzeder, A., Santner, J., Zhang, H., Prohaska, T., Wenzel, W.W., 2015. Uncertainty evaluation of the diffusive gradients in thin films technique. Environ. Sci. Technol. 49, 1594–1602.
Laird, D., Fleming, P., Wang, B., Horton, R., Karlen, D., 2010. Biochar impact on nutrient leaching from a midwestern agricultural soil. Geoderma 158, 436–442.
Larsen, M., Borisov, S.M., Grunwald, B., Klimant, I., Glud, R.N., 2011. A simple and inexpensive high resolution color ratiometric planar optode imaging approach: application to oxygen and pH sensing. Limnol. Oceanogr. Methods 9, 348–360.
Lu, S., Miller, M.H., 1993. Determination of the most efficient phosphorus placement for field-grown maize (*Zea mays* L.) in early growth stages. Can. J. Soil Sci. 73, 349–358.
Lützow, M.v., Kögel-Knabner, I., Ekschmitt, K., Matzner, E., Guggenberger, G., Marschner, B., Flessa, H., 2006. Stabilization of organic matter in temperate soils: mechanisms and their relevance under different soil conditions—a review. Eur. J. Soil Sci. 57, 426–445.
Magid, J., De Neergaard, A., Brandt, M., 2006. Heterogeneous distribution may substantially decrease initial decomposition, long-term microbial growth and n-immobilization from high C-to-N ratio resources. Eur. J. Soil Sci. 57, 517–529.
Mason, S.D., McLaughlin, M.J., Johnston, C., McNeill, A., 2013. Soil test measures of available P (colwell, resin and DGT) compared with plant P uptake using isotope dilution. Plant Soil 373, 711–722.
McLaren, R.G., Clucas, L.M., Speir, T.W., van Schaik, A.P., 2007. Distribution and movement of nutrients and metals in a *Pinus radiata* forest soil following applications of biosolids. Environ. Pollut. 147, 32–40.
Menzies, N.W., Kusumo, B., Moody, P.W., 2005. Assessment of P availability in heavily fertilized soils using the diffusive gradient in thin films (DGT) technique. Plant Soil 269, 1–9.
Mundus, S., Tandy, S., Cheng, H., Lombi, E., Husted, S., Holm, P.E., Zhang, H., 2011. Applicability of diffusive gradients in thin films for measuring Mn in soils and freshwater sediments. Anal. Chem. 83, 8984–8991.
Murphy, J., Riley, J.P., 1962. A modified single solution method for the determination of phosphate in natural waters. Anal. Chim. Acta 27, 31–36.
Peirce, C.A.E., Smernik, R.J., McBeath, T.M., 2013. Phosphorus availability in chicken manure is lower with increased stockpiling period, despite a larger orthophosphate content. Plant Soil 373, 359–372.
Popovic, M.O., Hjorth, M., Jensen, L.S., 2012. Phosphorus, copper and zinc in solid and liquid fractions from full scale and laboratory separated pig slurry. Environ. Technol. 33, 2119–2131.
Quiquampoix, H., Burns, R.G., 2007. Interactions between proteins and soil mineral surfaces: environmental and health consequences. Elements 3, 401–406.
Santner, J., Zhang, H., Leitner, D., Schnepf, A., Prohaska, T., Puschenreiter, M., Wenzel, W.W., 2012. High-resolution chemical imaging of labile phosphorus in the rhizosphere of *Brassica napus* L. cultivars. Environ. Exp. Bot. 77, 219–226.
Santner, J., Larsen, M., Kreuzeder, A., Glud, R.N., 2015a. Two decades of chemical imaging of solutes in sediments and soils — a review. Anal. Chim. Acta 878, 9–42.
Santner, J., Mannel, M., Burrell, L.D., Hoefer, C., Kreuzeder, A., Wenzel, W.W., 2015b. Phosphorus uptake by *Zea mays* L. is quantitatively predicted by infinite sink extraction of soil P. Plant Soil 386, 371–383.
Schröder, J.J., Vermeulen, G.D., van der Schoot, J.R., van Dijk, W., Huijsmans, J.F.M., Meuffels, G.J.H.M., van der Schans, D.A., 2015. Maize yields benefit from injected manure positioned in bands. Eur. J. Agron. 64, 29–36.
Six, L., Smolders, E., Merckx, R., 2013. The performance of DGT versus conventional soil phosphorus tests in tropical soils—maize and rice responses to P application. Plant Soil 366, 49–66.
Six, L., Smolders, E., Merckx, R., 2014. Testing phosphorus availability for maize with DGT in weathered soils amended with organic materials. Plant Soil 177–192.
Small, G.E., Bullerjahn, G.S., Sterner, R.W., Beall, B.F., Brovold, S., Finlay, J.C., McKay, R.M., Mukherjee, M., 2013. Rates and controls of nitrification in a large oligotrophic lake. Limnol. Oceanogr. 58, 276–286.
Sobek, A., Stamm, N., Bucheli, T.D., 2009. Sorption of phenyl urea herbicides to black carbon. Environ. Sci. Technol. 43, 8147–8152.
Sommer, S.G., Hjorth, M., Leahy, J., Zhu, K., Christel, W., Sørensen, C.G., Sutaryo, 2015. Pig slurry characteristics, nutrient balance and biogas production as affected by separation and acidification. J. Agric. Sci. 153, 177–191.

Spohn, M., Kuzyakov, Y., 2014. Spatial and temporal dynamics of hotspots of enzyme activity in soil as affected by living and dead roots—a soil zymography analysis. Plant Soil 379, 67–77.
Spokas, K., Koskinen, W., Baker, J., Reicosky, D., 2009. Impacts of woodchip biochar additions on greenhouse gas production and sorption/degradation of two herbicides in a Minnesota soil. Chemosphere 77, 574–581.
Spokas, K.A., Cantrell, K.B., Novak, J.M., Archer, D.W., Ippolito, J.A., Collins, H.P., Boateng, A.A., Lima, I.M., Lamb, M.C., McAloon, A.J., 2012. Biochar: a synthesis of its agronomic impact beyond carbon sequestration. J. Environ. Qual. 41, 973–989.
Stahl, H., Warnken, K.W., Sochaczewski, L., Glud, R.N., Davison, W., Zhang, H., 2012. A combined sensor for simultaneous high resolution 2-D imaging of oxygen and trace metals fluxes. Limnol. Oceanogr. Methods 10, 389–401.
Tandy, S., Mundus, S., Yngvesson, J., de Bang, T.C., Lombi, E., Schjørring, J.K., Husted, S., 2011. The use of DGT for prediction of plant available copper, zinc and phosphorus in agricultural soils. Plant Soil 346, 167–180.
Tsai, W., Liu, S., Chen, H., Chang, Y., Tsai, Y., 2012. Textural and chemical properties of swine-manure-derived biochar pertinent to its potential use as a soil amendment. Chemosphere 89, 198–203.
Uchimiya, M., Hiradate, S., 2014. Pyrolysis temperature-dependent changes in dissolved phosphorus speciation of plant and manure biochars. J. Agric. Food Chem. 62, 1802–1809.
Williams, P.N., Santner, J., Larsen, M., Lehto, N.J., Oburger, E., Wenzel, W., Glud, R.N., Davison, W., Zhang, H., 2014. Localized flux maxima of arsenic, lead, and iron around root apices in flooded lowland rice. Environ. Sci. Technol. 48, 8498–8506.
Wulf, S., Maeting, M., Clemens, J., 2002. Application technique and slurry co-fermentation effects on ammonia, nitrous oxide, and methane emissions after spreading. J. Environ. Qual. 31, 1795–1801.
Zhu, K., Christel, W., Bruun, S., Jensen, L.S., 2014. The different effects of applying fresh, composted or charred manure on soil N_2O emissions. Soil Biol. Biochem. 74, 61–69.
Zhu, K., Larsen, M., Glud, R.N., Bruun, S., Jensen, L.S., 2015. Heterogeneity of O_2 dynamics in soil amended with animal manure and implications for greenhouse gas emissions. Soil Biol. Biochem. 84, 96–106.
Zimmerman, A.R., Gao, B., Ahn, M., 2011. Positive and negative carbon mineralization priming effects among a variety of biochar-amended soils. Soil Biol. Biochem. 43, 1169–1179.